Gauge-Invariant Gravitational Wave Extraction from Coalescing Binary Neutron Stars

K. Oohara
Department of Physics, Niigata University, Niigata 950-2181, Japan

We report application of a method for extracting gravitational waves to three-dimensional numerical simulation on coalescing binary neutron stars. We found the extracted wave form includes the components corresponding to the quadrupole part in the Newtonian potential of the background metric, if it is monitored at a position not far from the central stars. We present how to eliminate it.

1. INTRODUCTION

We are constructing computer codes on three-dimensional numerical relativity [1, 2]. At first we used the conformal slicing condition, in which the metric becomes the Schwarzschild one in the outer vacuum region so that if the three-metric is split into the Schwarzschild background and the perturbed parts, the latter can be considered as the gravitational waves at the wave zone [3]. However, it has been found that this slicing involves unstable modes and long-term evolution of coalescing binary neutron star cannot be followed [1, 4]. Then we started to construct a new code using the maximal slicing condition. In this slicing, the perturbed part of the three-metric includes gauge dependent modes and therefore we need gauge-invariant wave extraction. Recently gauge-invariant wave extraction methods have been given as nonspherical perturbations of Schwarzschild geometry [5–8]. In this letter, we report application of a method based on them to three-dimensional general relativistic simulation on coalescing binary neutron stars.

2. BASIC EQUATIONS

We use (3+1)-formalism of the Einstein equation and write the line element as

$$ds^2 = -\alpha^2 dt^2 + \gamma_{ij}(dx^i + \beta^i dt)(dx^j + \beta^j dt). \tag{1}$$

Outside of the star, we split the total spacetime metric $g_{\mu\nu}$ into a Schwarzschild background and nonspherical perturbation parts:

$$g_{\mu\nu} = g^{(B)}_{\mu\nu} + h^{(e)}_{\mu\nu} + h^{(o)}_{\mu\nu}, \tag{2}$$

where $g^{(B)}_{\mu\nu}$ is the spherically symmetric metric given by

$$g^{(B)}_{\mu\nu} dx^\mu dx^\nu = -N^2 dt^2 + A^2 dr^2 + R^2(d\theta^2 + \sin^2\theta d\phi^2) \tag{3}$$

and $h^{(e)}_{\mu\nu}$ and $h^{(o)}_{\mu\nu}$ are even-parity and odd-parity metric perturbations, respectively;

$$h^e_{\mu\nu} = \sum_{lm} \begin{pmatrix} N^2 H_0 Y_{lm} & H_1 Y_{lm} & h^e_0 Y_{lm,\theta} & h^e_0 Y_{lm,\phi} \\ \star & A^2 H_2 Y_{lm} & h^e_1 Y_{lm,\theta} & h^e_1 Y_{lm,\phi} \\ \star & \star & h^e_{22} & R^2 G X_{lm} \\ \star & \star & \star & h^e_{33} \end{pmatrix} \tag{4}$$

$$h^e_{22} = R^2(K Y_{lm} + G W_{lm}) \tag{5}$$

$$h^e_{33} = R^2 \sin^2\theta \left(K Y_{lm} - G W_{lm}\right), \tag{6}$$

and

$$h^o_{\mu\nu} = \sum_{lm} \begin{pmatrix} 0 & 0 & -h^o_0 \dfrac{Y_{lm,\phi}}{\sin\theta} & h^o_0 Y_{lm,\theta}\sin\theta \\ 0 & 0 & -h^o_1 \dfrac{Y_{lm,\phi}}{\sin\theta} & h^o_1 Y_{lm,\theta}\sin\theta \\ \star & \star & \frac{R^2}{2} h^o_2 X_{lm}\sin\theta & -\frac{R^2}{2} h^o_2 W_{lm}\sin\theta \\ \star & \star & \star & -\frac{R^2}{2} h^o_2 X_{lm}\sin\theta \end{pmatrix} \tag{7}$$

where the symbol '$\star$' indicates the symmetric components, H_1, h^e_0, h^e_1, K, G, h^o_0, h^o_1, and h^o_2 are the functions of t and r for each l and m; Y_{lm} is the spherical harmonics, X_{lm} and W_{lm} are given by

$$X_{lm} = 2(Y_{lm,\theta\phi} - Y_{lm,\phi}\cot\theta), \tag{8}$$

$$W_{lm} = Y_{lm,\theta\theta} - Y_{lm,\theta}\cot\theta - Y_{lm,\phi\phi}/\sin^2\theta. \tag{9}$$

From the linearized theory about perturbations of the Schwarzschild spacetime, the gauge invariant quantities Ψ^o and Ψ^e are given by [9]

$$\Psi^o_{lm}(t,r) = \sqrt{2\Lambda(\Lambda-2)}N^2\left(\frac{h^o_1}{r} + \frac{r}{2}\frac{\partial h^o_2}{\partial r}\right) \tag{10}$$

and

$$\Psi^e_{lm}(t,r) = -\sqrt{\frac{2(\Lambda-2)}{\Lambda}}\ \frac{4r(N^2)^2 k_{2lm} + \Lambda r k_{1lm}}{\Lambda + 1 - 3N^2} \tag{11}$$

for the odd and even parity modes, respectively, where $\Lambda = l(l+1)$,

$$k_{1lm} = K + \Lambda G + 2N^2 r\frac{\partial G}{\partial r} - 2N^2\frac{h^e_1}{r} \tag{12}$$

and

$$k_{2lm} = \frac{H_2}{2N^2} - \frac{1}{2\sqrt{N^2}}\frac{\partial}{\partial r}\left[\frac{r}{\sqrt{N^2}}(K + \Lambda G)\right] \quad (13)$$

The quantities Ψ^o and Ψ^e satisfy the Regge-Wheeler and the Zerilli equations, respectively [10]. Two independent polarizations of gravitational waves h_+ and $h_\times$ are given by

$$h_+ - \mathrm{i}h_\times = \frac{1}{\sqrt{2}r}\sum_{l,m}(\Psi^e_{lm}(t,r) + \Psi^o_{lm}(t,r))_{-2}Y_{lm}, \quad (14)$$

where

$$_{-2}Y_{lm} = \frac{1}{\sqrt{\Lambda(\Lambda-2)}}\left(W_{lm} - \mathrm{i}\frac{X_{lm}}{\sin\theta}\right). \quad (15)$$

In numerical calculations, the functions $N^2(t,r)$, $A^2(t,r)$ and $R^2(t,r)$ of the background metric are calculated by performing the following integration over a two-sphere of radius r [7]:

$$N^2 = -\frac{1}{4\pi}\int g_{tt}\,\mathrm{d}\Omega, \quad A^2 = \frac{1}{4\pi}\int g_{rr}\,\mathrm{d}\Omega,$$

$$R^2 = \frac{1}{8\pi}\int\left(g_{\theta\theta} + \frac{g_{\phi\phi}}{\sin^2\theta}\right)\mathrm{d}\Omega, \quad (16)$$

where $\mathrm{d}\Omega = \sin\theta\mathrm{d}\theta\mathrm{d}\phi$. The components of the metric perturbations are

$$H_2(t,r) = \frac{1}{A^2}\int g_{rr}Y^*_{lm}\,\mathrm{d}\Omega, \quad (17)$$

$$G(t,r) = \frac{1}{\Lambda(\Lambda-2)}\frac{1}{R^2} \times \int\left[\left(g_{\theta\theta} - \frac{g_{\phi\phi}}{\sin^2\theta}\right)W^*_{lm} + \frac{2g_{\theta\phi}X^*_{lm}}{\sin^2\theta}\right]\mathrm{d}\Omega, \quad (18)$$

$$K(t,r) = \frac{1}{2}\Lambda G_{lm} + \frac{1}{2R^2}\int\left(g_{\theta\theta} + \frac{g_{\phi\phi}}{\sin^2\theta}\right)Y^*_{lm})\mathrm{d}\Omega, \quad (19)$$

$$h^e_1(t,r) = \frac{1}{\Lambda}\int\left(g_{r\theta}Y^*_{lm,\theta} + \frac{g_{r\phi}}{\sin\theta}\frac{Y^*_{lm,\phi}}{\sin\theta}\right)\mathrm{d}\Omega, \quad (20)$$

$$h^o_1(t,r) = -\frac{1}{\Lambda}\int\left(g_{r\theta}\frac{Y^*_{lm,\phi}}{\sin\theta} - \frac{g_{r\phi}}{\sin\theta}Y^*_{lm,\theta}\right)\mathrm{d}\Omega \quad (21)$$

and

$$h^o_2(t,r) = \frac{1}{2\Lambda(\Lambda-2)} \times \int\left[\left(g_{\theta\theta} - \frac{g_{\phi\phi}}{\sin^2\theta}\right)\frac{X^*_{lm}}{\sin\theta} - \frac{2g_{\theta\phi}}{\sin\phi}W^*_{lm}\right]\mathrm{d}\Omega, \quad (22)$$

where $*$ denotes the complex conjugate.

We need angular integrals over spheres for constant r, such as

$$F(r_0) = \int_{r=r_0} f(x,y,z)\mathrm{d}\Omega = \int f(r_0,\theta,\phi)\,\sin\theta\mathrm{d}\theta\mathrm{d}\phi. \quad (23)$$

If numerical simulation is performed using Cartesian coordinate system, we need interpolation to obtain the values of $f(r_0,\theta,\phi)$ from $f(x,y,z)$ at the grid points. It is, however, not easy to fully parallelize the procedure on a parallel computer with distributed memory. We therefore rewrite Eq.(23) as the volume integral, namely,

$$\begin{aligned} F(r_0) &= \frac{1}{r_0^2}\int f(x,y,z)\delta(r-r_0)\,\mathrm{d}^3x \quad (24) \\ &= \lim_{a\to 0}\frac{1}{\sqrt{\pi}ar_0^2}\int f(x,y,z)e^{-(r-r_0)^2/a^2}\,\mathrm{d}^3x, \end{aligned}$$

where $r = \sqrt{x^2+y^2+z^2}$. Numerical integral with $a = \Delta x/2$ gives a good value to Eq.(24), where Δx is the separation between grid points.

3. EXTRACTION OF GRAVITATIONAL WAVES

We have performed numerical simulation for a coalescing binary consisting of two identical neutron stars of mass $1.5M_\odot$ and evaluated the gravitational waves. The details of our code will be shown elsewhere [11] but it is essentially the same as Refs. [2] and [12]. The lapse function and the shift vector are determined by the maximal slicing and the pseudo-minimal distortion conditions, respectively. We used uniform $475 \times 475 \times 238$ Cartesian grid with $\Delta x = 1M_\odot$ assuming the symmetry with respect to the equatorial plane. As for an equation of state, we use the $\gamma = 2$ polytropic equation of state. The initial rotational velocity is given so that the circulation of the system vanishes. The ADM mass of the system is $2.8M_\odot$.

Figures 1 shows the evolution of density on the x-y plane. The stars start to coalesce at approximately $t = 0.5$msec and an almost axisymmetric star is formed by $t = 1.8$msec. Figure 2 shows the gravitational wave forms rh_+ and $rh_\times$ on the z-axis evaluated at $r = 110, 120, 130$ and $140M_\odot$ as functions of the retarded time $t-r$. Here $t = 0$ is the initial time of the numerical simulation. The lines of $rh_{+,\times}(t-r)$ estimated at $r = 110 \sim 140M_\odot$ for $t - r \gtrsim 0$ coincide with each other. Then the waves proportional to r^{-1} and propagating at the speed of light are extracted. For $t - r \lesssim 0$, however, lines of $rh_{+,\times}(t-r)$ do not coincide with each other. Then we plot $r^3h_{+,\times}$ as a function of t in Figure 3. In this figure, all the lines overlap each other for $t \lesssim 0.5$msec. It means that $h_{+,\times}$ includes a non-wave mode proportional to

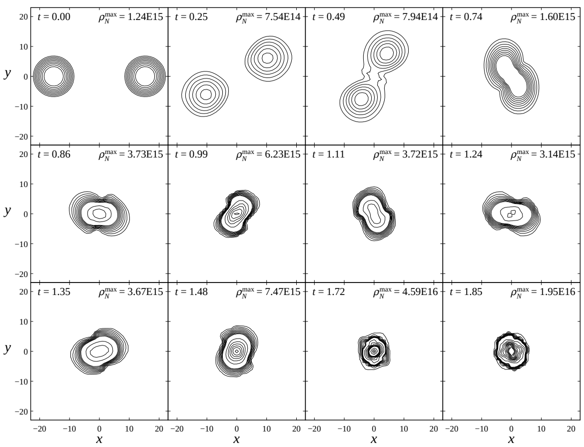

Figure 1: Density contour on the x-y plane. Time t in units of milliseconds and the maximum of density at each time are shown.

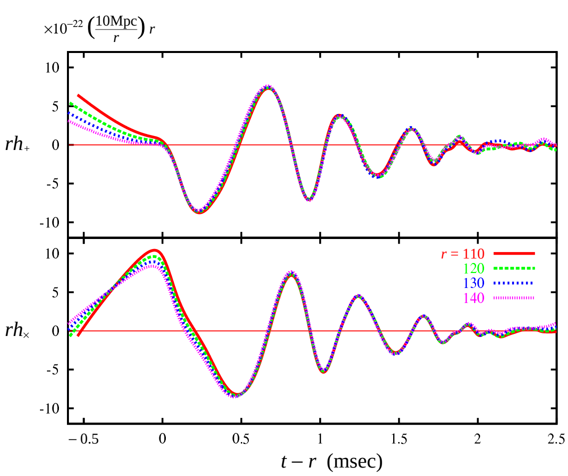

Figure 2: Plots $rh_{+,\times}$ along z-axis at $r = 110 \sim 140 M_\odot$ as a function of $t - r$.

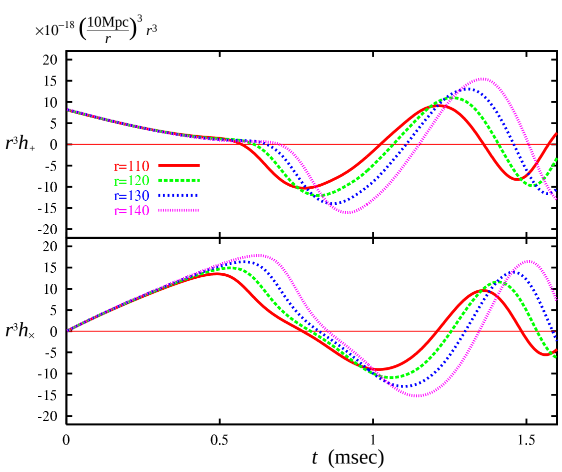

Figure 3: Plots $r^3 h_{+,\times}$ as a function of t.

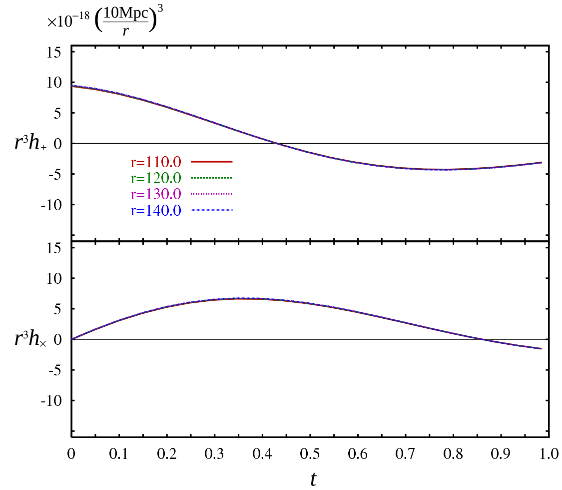

Figure 4: Plots $r^3 h_{+,\times}$ as a function of t for static point masses.

r^{-3}. This mode corresponds to the quadrupole part in the Newtonian potential of the background metric. As a matter of fact, a static star lying off-center produce non-zero h_+ and $h_\times$ although no waves are emitted. To evaluate the quantities of this mode, we put static point masses at the same position in Figure 1 and calculate $h_{+,\times}$. Figure /reffig:waves shows $r^3 h_{+,\times}$ evaluated at $r = 110 \sim 140 M_\odot$ as a function of t. It indicates that the non-wave mode dominates for small t and decrease fast as the merger of stars proceeds. For $t > r$, when the waves emitted at $t > 0$ in the central region arrive at the observer, the wave part dominate the none-wave part. Since this mode is proportional to r^{-3} while the wave mode is to r^{-1}, the former will be anyway negligible if the waves are monitored at a few times farther position.

Consequently $h_{+,\times}$ can be expressed as the sum of the wave part proportional to r^{-1} for each value of $t - r$ and the non-wave part proportional to r^{-3} for each value of t, that is

$$h(t, r) \equiv h_+ - \mathrm{i} h_\times = \frac{F(t-r)}{r} + \frac{G(t)}{r^3}. \tag{25}$$

In order to eliminate the non-wave part $G(t)/r^3$ and extract the wave part $F(t-r)/r$, we carry out the following procedure.

- Calculate the Fourier components $h_\omega(r)$ of $h(t, r)$ for each r. From Eq. (25), $h_\omega(r)$ can be written as

  $$h_\omega(r) = \frac{e^{-\mathrm{i}\omega r}}{r} F_\omega(r) + \frac{1}{r^3} G_\omega(r), \tag{26}$$

  where F_ω and G_ω are the Fourier components of $F(t)$ and $G(t)$, respectively, defined by

  $$F_\omega \equiv \frac{1}{2\pi} \int F(t) e^{-\mathrm{i}\omega t}\, \mathrm{d}t \tag{27}$$

and

$$G_\omega \equiv \frac{1}{2\pi}\int G(t)e^{-\mathrm{i}\omega t}\,\mathrm{d}t. \tag{28}$$

- From the values of $h_\omega(r)$ in different radial coordinates r_1 and r_2, F_ω can be given by

$$F_\omega = \frac{r_2^3 h_\omega(r_2) - r_1^3 h_\omega(r_1)}{r_2^2 e^{-\mathrm{i}\omega r_2} - r_1^2 e^{-\mathrm{i}\omega r_1}}. \tag{29}$$

- By inverse Fourier transformation, we can get the gravitational waves that do not include non-wave modes,

$$h_+(t,r) - \mathrm{i}h_\times(t,r) = \int \frac{e^{-\mathrm{i}\omega r}}{r}F_\omega e^{\mathrm{i}\omega t}\,\mathrm{d}\omega. \tag{30}$$

The resultant wave form is shown in Figure 5. The curves represent the average of h_+ and $h_\times$ calculated at $r = 110, 120, \cdots 200 M_\odot$ and twice the dispersion 2σ is shown as error bars.

Here we define $\widehat{h}_+$ and $\widehat{h}_\times$ as

$$\widehat{h}_+ = \frac{1}{2}(h_{xx} - h_{yy}) \quad \text{and} \quad \widehat{h}_\times = h_{xy}, \tag{31}$$

respectively, where $h_{ij} = \phi^{-4}\gamma_{ij} - \delta_{ij}$ and $\phi = (\det(\gamma_{ij}))^{\frac{1}{12}}$. The pseudo-minimal distortion condition demanding $\partial_t(\partial_j h_{ij}) = 0$ guarantees $\widehat{h}_{+,\times}$ to be transverse-traceless if $\partial_j h_{ij} = 0$ at $t = 0$. It is our case since we assumed the initial three-metric to be conformal flat, $h_{ij} = 0$. Then they can be considered as the gravitational waves on z-axis in the conformal slicing, while they include gauge dependent modes in the maximal slicing [3]. To compare $\widehat{h}_{+,\times}$ with $h_{+,\times}$ for the conformal slicing as well as for the maximal slicing, we have performed numerical simulation for a coalescing binary of two $M = 1.0M_\odot$ neutron stars. As shown in Figure 6, they almost coincide with each other, while a small deviation is found in $\widehat{h}_{+,\times}$ in the maximal slicing. Then we found that the gauge mode in $\widehat{h}_{+,\times}$ is small even in the maximal slicing.

Finally to investigate a possibility that the excitation of the quasi-normal modes can be seen by the numerically calculated waves, we evaluated the energy spectrum of the gravitational waves, which is given by

$$\frac{\mathrm{d}E_{\mathrm{GW}}}{\mathrm{d}\omega} = \frac{1}{32\pi}\sum_{l,m}\omega^2\left(\left|\Psi^{(e)}_{lm\omega}(r)\right|^2 + \left|\Psi^{(o)}_{lm\omega}(r)\right|^2\right), \tag{32}$$

where $\Psi^{(I)}_{lm\omega}(r)$ is the Fourier transformation of $\Psi^{(I)}_{lm}(t,r)$. Figure 7 shows the energy spectrum of the waves plotted in Figure 5. The fundamental frequency of $l = 2$ for the Schwarzschild black hole of mass $2.8M_\odot$ is $\omega = 25$ msec^{-1}. A peak near this frequency appears in Figure 7. Unfortunately, however,

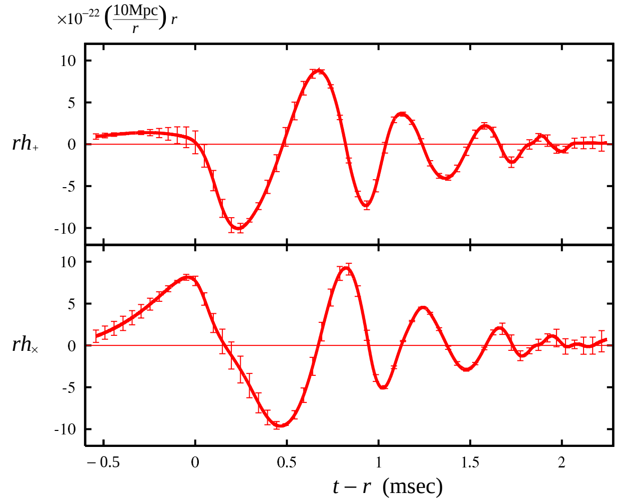

Figure 5: Wave forms $rh_{+,\times}$ along z-axis as a function of $t - r$. The curves are averages of $rh_{+,\times}$ estimated at $r = 110 \sim 200M_\odot$ and error bars denote 2σ.

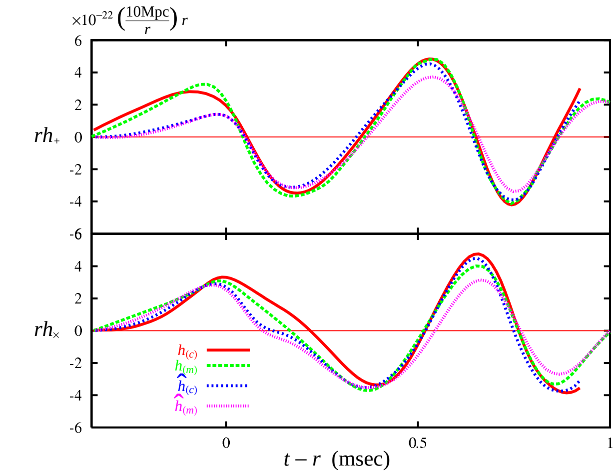

Figure 6: The comparison $h_{+,\times}$ defined by Eq.(30) and $\widehat{h}_{+,\times}$ defined by Eq.(31)) obtained with the conformal slicing (c) and the maximal slicing (m).

the rotating angular frequency just when the merger of the stars finishes is $12 \sim 15$ msec^{-1} and thus they will radiate the waves of frequency near $\omega = 25$ msec^{-1}. So that more precise calculation is necessary to discuss whether this peak corresponds to the emission of the quasi-normal mode of the formed black hole.

Acknowledgments

Numerical computations were carried out on SR8000/F1 at Hight Energy Accelerator Research Organization(KEK) and on VPP5000 at the Astronomical Data Analysis Center of the National Astronomical Observatory Japan(NAO). This work was in part supported by Grant-in-Aid for Scientific Research Pri-

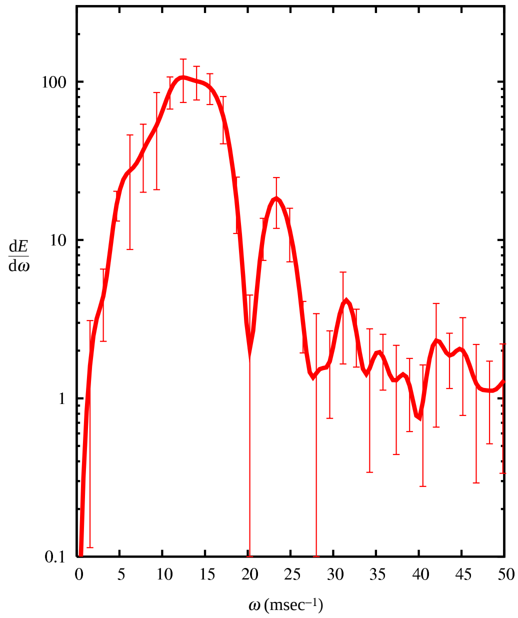

Figure 7: The energy spectrum of the gravitational waves plotted in Fig 5. The curves are averages of $\mathrm{d}E/\mathrm{d}\omega$ estimated at $r = 110 \sim 200M_{\odot}$ and error bars denote 2σ.

ority Area, No.16029205, from Japan Society for the Promotion of Science, by the Supercomputer Project of KEK and by the Large Scale Simulation Project of NAO.

References

[1] K. Oohara, T. Nakamura and M. Shibata, Prog. Theor. Phys. Suppl. No. 128 (1997), 183.
[2] K. Oohara and T. Nakamura, Prog. Theor. Phys. Suppl. No. 136 (1999), 270.
[3] M. Shibata and T. Nakamura, Prog. Theor. Phys. **88** (1992), 270.
[4] M. Shibata and T. Nakamura, Phys. Rev. **D52** (1995), 5428.
[5] A. Abrahams and C. Evans, Phys. Rev. **D36** (1988), 317.
[6] A. Abrahams and C. Evans, Phys. Rev. **D42** (1990) ,2585.
[7] A. Abrahams, D. Dernstein, D. Hobill and E. Seidel, Phys. Rev. **D45** (1992), 3544.
[8] A. Abrahams *et al.*, Phys. Rev. Lett. **80** (1998), 1812.
[9] V. Moncrief, Ann. Phys. (N.Y.) **88** (1974),322.
[10] F. J. Zerilli, Phys. Rev. Lett. **24** (1970), 737.
[11] M. Kawamura, K. Oohara and T. Nakamura, in preparation.
[12] K. Oohara and T. Nakamura, in *Proceedings of the Ninth Marcel Grossmann Meeting on General Relativity* ed. by V.G. Gurzdyan, R.T. Jantzen, R. Ruffini (World Scientific, Singapore, 2002) 2295.